Orientations of dipoles restricted by two oppositely charged walls

2007 J. Phys. A: Math. Theor. 40 11815

(http://iopscience.iop.org/1751-8121/40/39/008)

IOP Publishing Journal of Physics A: Mathematical and Theoretical

J. Phys. A: Math. Theor. **40** (2007) 11815–11826 doi:10.1088/1751-8113/40/39/008

Orientations of dipoles restricted by two oppositely charged walls

Stefano Maset[1] **and Klemen Bohinc**[2]

[1] Dipartimento di Matematica e Informatica, Universita 'di Trieste, 34100 Trieste, Italy
[2] University College for Health Studies, Poljanska 26a, University of Ljubljana, 1000 Ljubljana, Slovenia

E-mail: klemen.bohinc@fe.uni-lj.si

Received 24 February 2007, in final form 14 August 2007
Published 11 September 2007
Online at stacks.iop.org/JPhysA/40/11815

Abstract

We considered the system of two oppositely charged surfaces in a solution composed of dipoles and monovalent ions. The functional density theory for dipoles of arbitrary length was introduced. The spatial distribution of electric charge within the dipoles, the orientations of dipoles and their restrictions near the charged surface were taken into account. The result of the variational procedure gave the nonlinear integro-differential equation for the electrostatic potential. It was numerically solved by restating it as a fixed-point equation in an infinite-dimensional space of functions and then by looking for an approximated solution in the finite-dimensional space of functions defined in a mesh of Chebyshev nodes. The numerical solution showed that the dipoles are predominantly oriented parallel to the electric field, i.e. perpendicular to the charged surfaces. The interaction between oppositely charged surfaces mediated by dipoles was discussed.

PACS numbers: 41.20.Cv, 46.70.Hg, 82.45.Un

1. Introduction

Biological structures are normally composed of a large number of charged groups. Biopolymers (DNA, polyelectrolytes, polystyrene sulfonate), membranes, cellular components or globular proteins behave electrically as sets of point charges at fixed positions on the molecules [1–3]. Normally, these structures are inserted in the biological medium where besides the water molecules the free ions are also present. The ions can be counterions, which are attracted by charged objects of opposite sign, or coions, which are depleted by the charged objects of the same sign [4]. Therefore, the electrostatic interactions between charged objects in soft and biological matter play an important role; they can be both attractive and repulsive.

The biological processes may take place between surfaces that are not equally charged and even oppositely charged [5, 6]. Such situations have recently been studied in protein association with DNA and membranes [7], the interaction between cationic liposomes and negatively charged cell membranes [7, 8] and DNA association with artificial cationic liposomes [9, 10]. In these situations macroions are charged surfaces of membranes, DNA and proteins.

Many molecules are dipoles due to non-uniform distribution of positive and negative charges on the various atoms. Dipoles are characterized by their dipole moment, a vector quantity with the magnitude equal to the product of the positive charge and the distance separating the two charges of the dipole [11]. A novel method was developed for the preparation of the colloid particles with dipolar charge distribution [12, 13]. The peptide chains can be organized into α-helices or β-sheets which also possess dipole moment [14–16]. In these structures, the vector summation of all constituent dipole moments can lead into a large total dipole moment.

Recently, the electrostatic interactions between strongly charged objects (macroions) in aqueous solutions pay large interest. The first approach to describe such systems is the mean-field Poisson–Boltzmann (PB) theory [17, 18], where the particles in the solution are treated as dimensionless, the correlations between the particles are not taken into account, the solution is accounted for by the dielectric constant and the surfaces of macroions are uniformly charged. Approaches were proposed where the correlations between the particles are incorporated: integral-equation theories [19, 20], perturbative expansions around the mean-field PB theory [21, 22] and local density functional theories [23]. The finite size of ions was taken into account [24–26]. A spatially distributed charge within multivalent ions was considered [27]. To check the theoretical results, the Monte Carlo simulations have been performed [28–30].

The orientation of dipoles near the charged surfaces has also been studied. Lamperski *et al* [31] used the improved PB theory for mixture of hard spheres with either point electric charges or point electric dipole moments embedded at their centers. Monte Carlo and molecular dynamics simulations [32, 33] have been performed to characterize the structure of dipoles at charged surfaces.

In this work, we developed a density functional theory for the case of arbitrary long dipoles sandwiched between two oppositely charged surfaces. In the solution we added also positive and negative monovalent ions. The internal structure of each dipole is accounted for and the intra-dipole correlations are taken into account. Our description of the charge distribution within a single dipole goes beyond the standard approach of macroscopic electromagnetism. We did not use Taylor expansion to describe the average charge density within a single dipole; in contrast we have used the exact expression for the charge density within a single dipole.

In the following sections, we first derive a theory that considers the charge distribution of individual dipoles and monovalent ions. The positional and orientational degrees of freedom for rod-like dipoles are taken into account. The restriction of dipole orientations near the hard charged walls is taken into account. The water molecules in the solution are accounted for by the dielectric constant. The equation for electrostatic potential is the integro-differential equation, which was solved numerically. In section 3, the novel numerical method is described, which approach consists of the discretization of an infinite-dimensional space of functions into a finite-dimensional space, reducing the integro-differential equation to a system of nonlinear algebraic equations. The solution of the system by an iterative numerical method requires, at every step of iteration, the solution of a boundary value problem of ordinary differential equation. In section 4, we present the results of the numerical calculations, i.e. the profile of electrostatic potential, the profile of electric field strength, the profile of volume charge density, the spatial distribution of monovalent ions, the spatial distribution of the reference

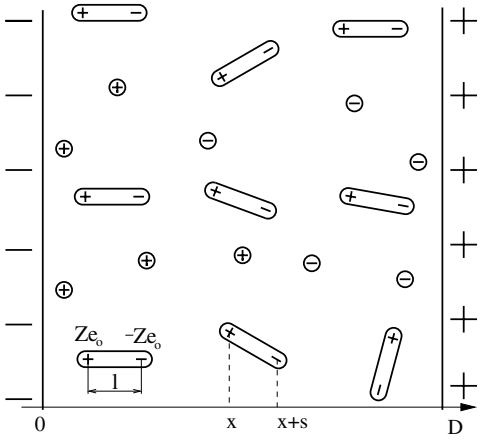

Figure 1. Schematic presentation of two oppositely-charged planar surfaces, which is filled with water containing dipoles with dipole moment Ze_0l and monovalent positive and negative ions. The separation between the individual charges of each dipole is denoted by l. The valency of each charge of the dipole is Z.

charges of dipoles and their orientations within the solution. In the last section, the influence of dipoles on the interaction between oppositely charged surfaces is discussed.

2. Theory

In this work, we formulate the density functional theory for an aqueous solution containing dipoles and monovalent ions. The dipoles have internal structure, each dipole is composed of negative and positive elementary charges of valency Z, separated by a distance l, i.e. the dipole moment of each dipole is Ze_0l, where e_0 is the elementary charge. The solution is sandwiched between the two large planar, oppositely charged surfaces (figure 1). Each surface bears an absolute value of surface charge density σ. The distance between the two surfaces is D.

We assume that there is no electric field behind the charged plates. The electrostatic field varies only in the normal direction between the two plates (x-direction). The dipoles are characterized by the positional and the orientational degrees of freedom while the monovalent ions are characterized only by the positional degree of freedom. We describe the dipole by referring to the positive charge as a reference charge, denoting the local concentration of all the reference charges by $n(x)$. The location of the negative charge of a given dipole is specified by the conditional probability density $p(s|x)$, denoting the probability to find the negative charge at position $(x + s)$ if the positive is at x. At any given position x, we require the normalization condition $\frac{1}{2l}\int_{-l}^{l} \mathrm{d}s p(s|x) = 1$ to be fulfilled. Note also that $p(s|x) = 0$ for $|s| > l$.

The free energy of the system per unit area of the plate A and the thermal energy kT is composed of the energy stored in the electrostatic field, the translational and the orientational entropy of the dipoles as well as the translational entropy of the monovalent ions,

$$\frac{F}{AkT} = \frac{1}{8\pi l_B}\int_0^D \mathrm{d}x\, \Psi'(x)^2 + \int_0^D \mathrm{d}x[n(x)\ln v_0 n(x) - n(x)] + \int_0^D \mathrm{d}x\, n(x)\frac{1}{2l}\int_{-l}^{l} \mathrm{d}s\; p(s|x)[\ln p(s|x) + U(x,s)]$$

$$+\int_0^D \mathrm{d}x\, n(x)\lambda(x)\left[\frac{1}{2l}\int_{-l}^{l}\mathrm{d}s\; p(s|x)-1\right]+\mu\int_0^D \mathrm{d}x\left[n(x)-\frac{N}{AD}\right]$$
$$+\int_0^D \mathrm{d}x\sum_{i=\{+,-\}}\left[n_i(x)\ln\frac{n_i(x)}{n_{0s}}-(n_i(x)-n_{0s})\right], \tag{1}$$

where $\Psi=\frac{e_0\phi}{kT}$ is the reduced electrostatic potential, ϕ is the electrostatic potential, μ is the reduced chemical potential, v_0 is the volume of the dipole, $l_\mathrm{B}=e_0^2/4\pi\epsilon\epsilon_0 kT$ is the Bjerrum length, ϵ is the dielectric constant of water, ϵ_0 is the influence constant, k is the Boltzmann constant, T is the absolute temperature, N is the number of dipoles, n_i is the concentration of the monovalent ions of the ith type and n_{0s} is the bulk concentration of monovalent ions. The sum in equation (1) runs over positive '$i=+$' and negative '$i=-$' monovalent ions. The Lagrange parameter λ ensures the normalization condition for the conditional probability density. The fifth term in equation (1) ensures the constant number of dipoles in the solution. We introduce the external reduced potential of the charged wall

$$U(x,s)=\begin{cases}0, & x>0 \quad \text{and} \quad x+s>0 \quad \text{and} \quad x<D \quad \text{and} \quad D-x-s>0\\ \infty, & \text{elsewhere,}\end{cases}$$

which ensures that the dipoles could not penetrate through the charged wall.

In thermal equilibrium, the free energy $F=F[n(x),p(s|x),n_i(x)]$ is minimal with respect to the functions $n(x)$, $p(s|x)$ and $n_i(x)$. The variational procedure ($\delta F=0$) gives the local concentration of monovalent ions

$$n_i(x)=n_{0s}\,\mathrm{e}^{-\mathrm{i}\Psi(x)}, \tag{2}$$

the conditional probability density

$$p(s|x)=\frac{\mathrm{e}^{-U(x,s)+Z\Psi(x+s)}}{q(x)} \tag{3}$$

and the local concentration of reference charges of dipoles

$$n(x)=n_0\,\mathrm{e}^{-Z\Psi(x)}q(x), \tag{4}$$

where $n_0=\frac{1}{v_0}\,\mathrm{e}^{-\mu}$ is the concentration of reference charges at vanishing electrostatic ($\Psi=0$) and external ($U=0$) potentials, and

$$q(x)=\frac{1}{2l}\int_{-l}^{l}\mathrm{d}s\,\mathrm{e}^{-U(x,s)+Z\Psi(x+s)} \tag{5}$$

is the orientational partition function of a single dipole with the position of its reference charge at x. In equation (4), the term $\mathrm{e}^{-Z\Psi(x)}$ corresponds to the Boltzmann distribution for the concentration of the reference charges of dipoles.

The local charge density has contributions from positive reference charges that are located at x and from the orientational mobile negative charges, located at $(x-s)$ with the corresponding probability density $p(s|x-s)$ as well as from the positive and negative charges of monovalent ions. Inserting the local charge density

$$\frac{\rho(x)}{e_0}=Zn(x)-Z\frac{1}{2l}\int_{-l}^{l}\mathrm{d}s\, n(x-s)p(s|x-s)+\sum_{i=\{+,-\}}\mathrm{i}n_i(x) \tag{6}$$

into the Poisson equation $\Psi''(x)=-4\pi l_\mathrm{B}\frac{\rho(x)}{e_0}$, we obtain the integro-differential equation for the reduced electrostatic potential

$$\Psi''(x)=8\pi l_B Z n_0\frac{1}{2l}\int_{\max[-l,-x]}^{\min[l,D-x]}\mathrm{d}s\,\sinh[Z\Psi(x)-Z\Psi(x+s)]+8\pi l_B n_{0s}\sinh[\Psi(x)]. \tag{7}$$

The boundary conditions are given at the charged plates

$$\Psi'(x=0) = -\sigma\frac{4\pi l_B}{e_0}, \tag{8}$$

$$\Psi'(x=D) = -\sigma\frac{4\pi l_B}{e_0}. \tag{9}$$

These boundary conditions demand a neutral overall charge for the system [34].

In the case of the solution composed of only monovalent ions ($n_0 = 0$, the dipoles are not present) the integro-differential equation (7) reduces to the well-known PB equation for the monovalent salt of ions $\Psi''(x) = 8\pi l_B n_{0s}\sinh[\Psi(x)]$.

If the electrostatic potential is small compared to the thermal energy ($\Psi \ll 1$) then in equation (7) we can linearize the term $\sinh[Z\Psi(x) - Z\Psi(x+s)]$ to $Z\Psi(x) - Z\Psi(x+s)$ and the term $\sinh[\Psi(x)]$ to $\Psi(x)$. The linearized integro-differential equation is

$$\Psi''(x) = 8\pi l_B Z n_0 \frac{1}{2l}\int_{\max[-l,-x]}^{\min[l,D-x]} \mathrm{d}s[Z\Psi(x) - Z\Psi(x+s)] + 8\pi l_B n_{0s}\Psi(x). \tag{10}$$

with the same boundary conditions (8) and (9).

3. Numerical method

The analytical solution of the integro-differential equation (7) with boundary conditions (8) and (9) is not available. A numerical solution is obtained in the following way. The integro-differential boundary value problem is restated as a fixed-point equation

$$\Psi = \mathcal{F}(\Psi), \tag{11}$$

where $\mathcal{F}(\Psi)$ is the solution Φ of the ordinary differential boundary value problem

$$\Phi''(x) = 8\pi l_B Z n_0 \frac{1}{2l}\int_{\max[-l,-x]}^{\min[l,D-x]} \mathrm{d}s\sinh[Z\Phi(x) - Z\Psi(x+s)] + 8\pi l_B n_{0s}\sinh[\Phi(x)], \tag{12a}$$

$$\Phi'(x=0) = -\sigma\frac{4\pi l_B}{e_0}, \tag{12b}$$

$$\Phi'(x=D) = -\sigma\frac{4\pi l_B}{e_0}. \tag{12c}$$

The fixed-point equation (11) is then discretized by replacing the domain $[0, D]$ of equation (7) by a mesh of N Chebyshev nodes, the function Ψ by an N-dimensional vector Ψ_N of values at the mesh nodes and equation (11) by the finite-dimensional algebraic equation

$$\Psi_N = \pi_N(\mathcal{F}(p_N(\Psi_N))), \tag{13}$$

where $p_N(\Psi_N)$ is the polynomial interpolating the values in the vector Ψ_N at the mesh nodes and $\pi_N(\Phi)$ is the N-dimensional vector of the values of the function Φ at the mesh points.

For the numerical computation we use MATLAB software. The discretized fixed-point equation (13) is rewritten as

$$G(\Psi_N) = \Psi_N - \pi_N(\mathcal{F}(p_N(\Psi_N))) = 0 \tag{14}$$

and then solved by the 'fsolve' MATLAB function (present in the optimization toolbox), which finds solutions of nonlinear algebraic equations by a least-squares method.

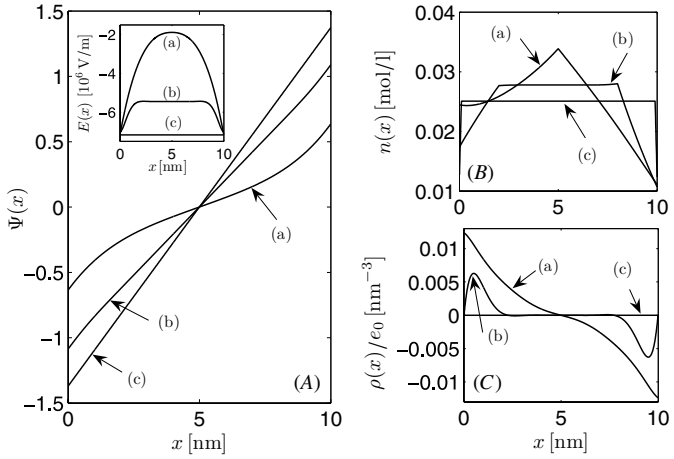

Figure 2. Linearized theory. Salt of monovalent ions is not present. (*A*) Reduced electrostatic potential $\Psi(x)$ and electric field strength $E(x)$ (in inset), (*B*) local concentration of reference charges $n(x)$ and (*C*) charge density $\rho(x)$ as a function of the distance from the left charged plate x. The lengths of dipoles $l = 5$ nm (a), $l = 2$ nm (b) and $l = 0.1$ nm (c) are shown. The volume of dipole is $v_0 = la_0$. The model parameters are $D = 10$ nm, $a_0 = 1$ nm^2, $\sigma = 0.005$ As m^{-2}, $Z = 1$, $\epsilon = 78$, $T = 300$ K and $N = 25$ for $A = 100$ nm^2.

The function 'fsolve' requires the computation of values of G, and so it requires the solution of the second-order ordinary boundary value problems of equation (12). Such problems are restated as first-order equations and then solved by the 'bvp4c' MATLAB function, which finds the solution of two-point ordinary boundary value problems by collocation. Finally, the integral in equation (12*a*) is computed by the 'quad' MATLAB function.

4. Results

Figure 2(*A*) shows the reduced electrostatic potential Ψ and the electric field strength E (in the inset) as a function of the distance from the left charged plate x between two oppositely charged plates for three different lengths of dipoles. The electrostatic potential Ψ monotonously increases with increasing distance from the left charged surface. The electric field strength E is symmetric with respect to the midplane of the system. In the limit of very small dipoles the electrostatic potential reduces to the electrostatic potential of the condenser filled with water, the electric field strength becomes constant $E_0 = -7.1 \times 10^6$ V m^{-1}. The difference between the field strength and the constant value E_0 increases with increasing lengths of dipoles.

Figure 2(*B*) shows the concentration of reference charges n and figure 2(*C*) shows the charge density ρ as a function of the distance from the left charged plate x between two equally charged plates for three different lengths of dipoles. The concentration of reference charges n first increases, reaches maximum value and then decreases with increasing x. In the limit $l = 0$ the concentration n has a constant value. The local concentration of reference charges $n(x)$ is not smooth (figure 2(*B*)). The first derivative of $n(x)$ is discontinuous at $x = l$ and $x = D - l$. In the regions $0 < x < l$ and $D - l < x < D$ the orientational restriction of dipoles is present. In the region $l < x < D - l$ the orientational restriction of dipoles is not present. For longer dipoles l the absolute value of charge density ρ decreases with increasing distance from the left charged surface. For smaller l the absolute value of charge density ρ first

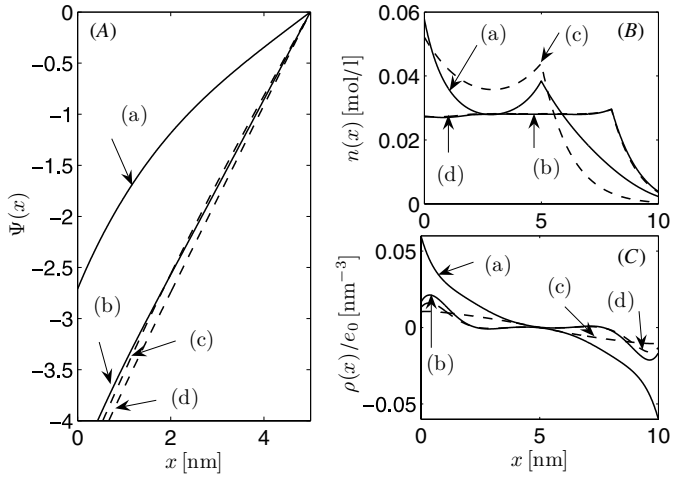

Figure 3. Comparison between the nonlinearized (full lines) and the linearized (dashed lines) theories. Salt of monovalent ions is not present. (*A*) Reduced electrostatic potential Ψ, (*B*) local concentration of reference charges n and (*C*) charge density ρ as a function of the distance from the left charged plate x for two different lengths of dipoles $l = 5$ nm (a, c) and $l = 2$ nm (b, d). The volume of each dipole is $v_0 = la_0$. The model parameters are $D = 10$ nm, $a_0 = 1$ nm^2 and $\sigma = 0.02$ As m^{-2}, $Z = 1$, $\epsilon = 78$, $T = 300$ K and $N = 25$ for $A = 100$ nm^2.

increases, reaches a maximum and then decreases with increasing distance to the zero value in the center of the system. In the limit of very small dipoles the charge density vanishes.

The comparison between the nonlinearized and the linearized theories is shown in figure 3 for the surface charge density $\sigma = 0.02$ As m^{-2}. The absolute value of the potential obtained with the linearized theory is larger than the absolute value of the potential obtained with the nonlinearized theory (figure 3(*A*)). This difference increases with increasing l. Near the charged surfaces the concentration of reference charges obtained within the nonlinearized model is larger than the concentration calculated within the linearized theory (figure 3(*B*)). There is a tiny difference between the nonlinearized and linearized theories for $l = 2$ nm (see curves (b) and (d) in figure 3(*B*)). This difference increases with increasing l. In the region $0 < x < 5$ nm the charge density of the nonlinearized theory is larger than the charge density of the linearized theory, while in the region 5 nm $< x <$ 10 nm opposite behavior is obtained (figure 3(*C*)).

The presence of the monovalent salt in the solution has an influence on the radial distribution of dipoles near the charged surfaces. Figure 4 shows (A) the reduced electrostatic potential Ψ, (B, C) the concentration of reference charges of dipoles n and the concentration of negative monovalent ions n_- as a function of the distance from the left charged plate x between two oppositely charged plates for three different bulk salt concentrations. We see that the presence of monovalent salt decreases the absolute value of the potential. This effect is pronounced for increasing bulk concentration of monovalent counterions and coions. The presence of the salt monovalent ions also has an influence on the concentration of reference charges of dipoles. With increasing bulk value n_{0s} of monovalent salt the concentration of reference charges of dipoles n near the negatively charged surfaces decreases, while near the positively charged surfaces the concentration n increases. In the mid-plane of the system there is a tiny influence of n_{0s} on the concentration of reference charges $n(x)$. For larger n_{0s} the result of the PB theory for monovalent salt (without dipoles) is reached (figure 4(*C*)).

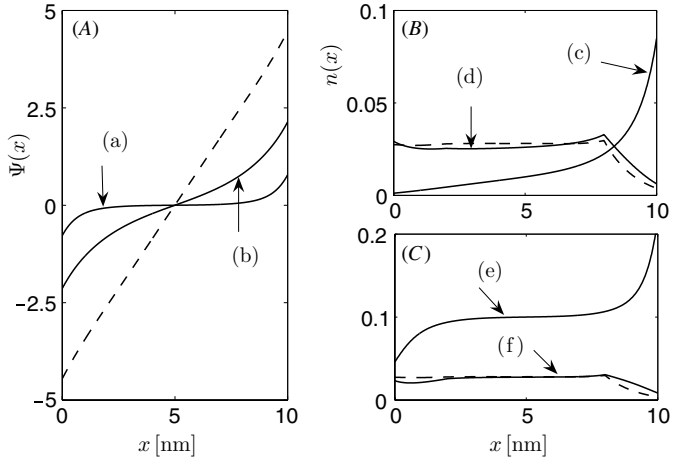

Figure 4. Nonlinearized theory, salt of monovalent ions included. (*A*) Reduced electrostatic potential $\Psi(x)$ as a function of the distance from the left charged plate x for three different bulk concentrations of monovalent ions $n_{0s} = 0.1$ mol l^{-1} (a), $n_{0s} = 0.01$ mol l^{-1} (b) and $n_{0s} = 0$ (dashed line). (*B*, *C*) local concentrations of reference charges $n(x)$ (d, f) and concentration of negative monovalent salt ions $n_-(x)$ (c, e) as a function of the distance from the left charged plate x. The bulk concentrations are $n_{0s} = 0.01$ mol l^{-1} (B) and $n_{0s} = 0.1$ mol l^{-1} (C). All dashed lines are given for $n_{0s} = 0$. The lengths of dipoles is $l = 2$ nm. The volume of dipole is $v_0 = la_0$. The model parameters are $D = 10$ nm, $a_0 = 1$ nm^2, $\sigma = 0.02$ As m^{-2}, $Z = 1$, $\epsilon = 78$, $T = 300$ K and $N = 25$ for $A = 100$ nm^2.

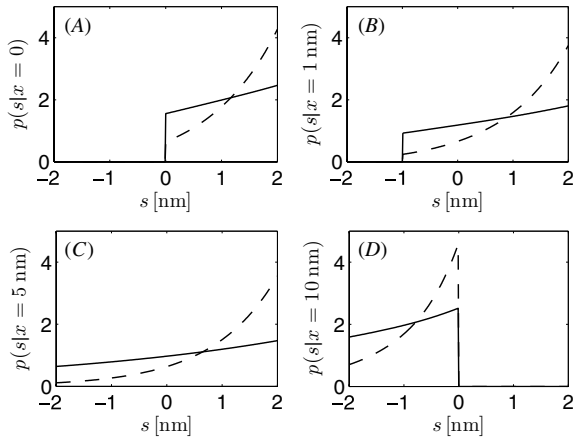

Figure 5. Conditional probability density as a function of the projection of the dipoles with respect to the axis x for four different coordinates of the reference charge (*A*) $x = 0$, (*B*) $x = 1$ nm, (*C*) $x = 5$ nm and (*D*) $x = 10$ nm. The surface charge densities are $\sigma = 0.005$ As m^{-2} (full lines) and $\sigma = 0.02$ As m^{-2} (dashed lines). The volume of dipole is $v_0 = la_0$. The nonlinear theory is used. The model parameters are $l = 2$ nm, $D = 10$ nm, $a_0 = 1$ nm^2 and $Z = 1$ and $N = 25$ for $A = 100$ nm^2.

Figure 5 shows the conditional probability density $p(s|x)$ as a function of the projection s of dipoles to the x direction. Two different surface charge densities are given for the dipoles of length $l = 2$ nm. We use the nonlinearized modified PB theory. The calculation is made

for reference charges located at coordinates $x = 0$, $x = 1$ nm, $x = 5$ nm and $x = 10$ nm. In the interval $0 < x < 2$ nm the conditional probability densities are defined only in the interval $-x < s < l$, while in the interval 8 nm $< x <$ 10 nm the conditional probability densities are defined in the interval $-l < s < D - x$. The conditional probability density increases with increasing s. For $x = 0$, $x = 1$ nm and $x = 5$ nm the conditional probability density reaches its maximum at $s = +l$, while for $x = 10$ nm the conditional probability density reaches its maximum at $s = D - x$.

5. Discussion

In summary, we considered two charged surfaces of opposite sign which are filled with aqueous solution of dipoles and monovalent ions. For such a system we introduced the density functional theory which enables us to study the spatial and the orientational distributions of dipoles. We showed that the dipoles tend to be oriented parallel to the electric field.

First, we discuss the concentration profile of reference charges of dipoles and the volume charge density. For small dipoles, the concentration of reference charges (positive charges) of dipoles close to the charged surfaces is small (figure 2(*B*)). The decrease of concentration n close to the charged surfaces compared to n in the center of the system can be attributed to the finite dimension of dipoles in a small region in the vicinity of the charged surfaces. Namely, the charged surfaces restrict the orientations of the dipoles leading to decreased concentration n close to the charged surfaces. On contrary, the dipoles with reference charges in the midplane can take all possible orientations. This is the reason why the concentration n in the midplane of the system is larger than the concentration n near the charged surfaces. The decrease in the concentration of reference charges near the charged surfaces is nonsymmetric. The concentration of reference charges is larger close to the negatively charged surface compared to the positively charged surface. The reason is the attraction (repulsion) between the negatively (positively) charged surfaces and the reference charges of dipoles. This means that the volume charge density near the negatively charged surface takes positive values, while the volume charge density near the positively charged surface takes negative values (figure 2(*C*)). The charge density is antisymmetric with respect to the midplane of the system indicating that both walls restrict the orientation of the dipoles in the same way. The volume charge density characterizes the total probability to find the dipoles with reference charges positioned at x. In the center, the positive and negative charges of dipoles are present with equal probabilities and the charge density is zero.

We also discuss the conditional probability density (figure 5). We showed that the dipoles prefer to be oriented perpendicular to the charged surface, i.e. the dipoles orient parallel to the electric field. This preference of the orientations is enhanced by increasing surface charge density. Namely, the increasing surface charge density increases their electrostatic interaction with the charges of the dipoles. Let us note that if we force the positive reference charges to sit at the positive charged surface then the dipoles are oriented parallel to the charged surface (figure 5(*D*)). These situations happen very rarely and can be excluded in the discussion, because the concentration of reference charges near the positively charged surface is negligible.

Here, we introduce two examples which indicate that the orientation of dipoles is influenced by the electric field of the charged surface. It was shown that the orientation of the IgG protein near the charged sorbent surface can be strongly influenced by electrostatic interactions [35, 36]. The orientation of polarized ions around the DNA molecule was also measured [37].

The dipoles have influence on the electric field strength E in the solution (figure 2(A)). The electric field strength varies with the distance from the surface and is perpendicular to the charged surfaces. Near the charged surfaces there is a small influence of the dipole length l on E, while in the center of the system there is a large influence of the dipole length l on E. For a given l the electric filed strength E exhibits the largest variation with respect to the x-axis close to the charged surfaces. This behavior was experimentally observed [38]. The increasing lengths of dipoles decreases the absolute value of the electric field strength. In the limit of very small dipoles the electric field strength is equal to the electric field strength of the condenser $E = -\frac{\sigma}{\epsilon\epsilon_0}$ [11].

In our case, the electric field of the system is produced by the charged surfaces and dipoles in the solution. The dipoles possess the dipole moment. In the external electric field the dipoles orient in the direction of the electric field in order to decrease the electric field between the surfaces. This phenomenon lowers the electric field strength between the surfaces. Our calculation shows that the dipoles are aligned along the electric field, because the conditional probability density shows that the most probable orientation of dipoles corresponds to the orientation parallel to the electric field strength. The degree of the alignment is determined by the temperature and the surface charge density of the system. Also the steric restrictions near the charged surface have influence on the dipole orientation.

We showed that the presence of the monovalent salt in the solution has an influence on the distribution of dipoles. The positive monovalent ions are attracted by the negatively charged surface and can be understood as the counterions for negatively charged surface (see figures 4(B), (C)). Similarly, the negative monovalent ions are attracted by the positively charged surfaces and can be understood as counterions for the positively charged surface (see figures 4(B), (C)). With increasing salt concentration near the negatively (positively) charged surface, the concentration of reference charges $n(x)$ decreases (increases). This phenomenon can be explained by the screening of charged surfaces via counterions. Namely, the positive (negative) ions screen the negatively (positively) charged surface. The negatively charged surface becomes less attractive for the reference charges of dipoles, while the positively charged surface becomes more attractive for the reference charges. In the center of the solution, the concentration of positive and negative ions is the same and influence of the salt on the distribution $n(x)$ is negligible. In the limit of very small concentration of dipoles the potential profile converges to the usual PB equation for monovalent salt.

In our model we adopted some simplifications. We did not take into account the correlations between dipoles in solution [20, 28, 39]. But the intra particle correlation within one dipole has been accounted for by spatial separation of the charges within the dipole. Also we did not take into account the correlations between the dimensionless monovalent ions. Namely, the PB theory yields satisfactory agreement with the computer simulations for solutions with monovalent counterions [18, 40]. We did not consider the partial adsorption of dipoles on the charged plate [41, 42].

Our system is composed of two oppositely charged surfaces and the dipoles, which have two oppositely signed charges. The overall charge of the system vanishes $\int_0^D \rho(x)\,\mathrm{d}x A = 0$. The two surfaces are electro-neutral and each dipole is electro neutral. Therefore the electro-neutrality is guaranteed for any number of dipoles. The number of dipoles in the solution is fixed through the constraint given in the fifth term of the free energy (equation (1)). We consider the cube of surface area $A = 100\ \mathrm{nm}^2$ and the distance between the charged surfaces $D = 10$ nm which corresponds to the volume $V_c = 1000\ \mathrm{nm}^3$. In this cube, we chose $N = 25$ dipoles. This means that each dipole with length l can approximately occupy $40\ \mathrm{nm}^3$. For the given l the approximate volume can be obtained as $v_c = \frac{4\pi(l/2)^3}{3}$. This simple consideration

limits the maximal lengths of dipoles to $l_c = 4$ nm and substitutes the incorporation of the steric effects in the theory.

Figures 2 and 3 also show the results for the dipoles of length $l = 5$ nm, which lies on the border of the validity. The results for $l = 5$ nm indicate that too long dipoles could create non-real values of concentrations and volume charge densities (see figures 2(*B*), (*C*)). The volume charge density (figure 2(*C*)) for dipoles of $l = 5$ nm have a completely different behavior as the volume charge density for the dipoles of length $l = 2$ nm.

The difference between the linearized and nonlinearized theories becomes important for larger surface charge densities. We estimated that above the surface charge density $\sigma = 0.01$ As m^{-2} the deviation of the linearized theory with respect to the nonlinearized theory is observed. The linearized theory predicts a larger absolute value of the potential and smaller concentrations of reference charges near the charged surface. These observations are similar to the observations for monovalent ions [26].

Like any approximations, the PB theory and our density functional theory have limits of validity. Under physiological conditions, electrolyte strength around 0.1 mol l^{-1}, it describe rather well the ionic distributions as long as the surface is not too highly charged [3, 18]. The PB theory can be applied only to the objects if $l_B \ll a$, where a is the typical radius of the object.

In principle, our equation can be solved for given boundary conditions, which can be either the Dirichlet boundary condition (the constant surface potential) or the Neumann boundary condition (the constant surface charge density) [17, 18]. The two boundary conditions are the limiting cases of the boundary condition where the fraction of the dissociated ionizable surface groups is treated as a self-consistent functional of the electrostatic potential [43]. In the majority of the biological relevant cases the surface density can be kept constant [3]. Therefore, in our calculation we used the Neumann boundary condition with fixed surface charge density (equations (8), (9)).

The presence of the dipoles in the electrolytes solution has the influence on the interaction between two oppositely charged surfaces. The force between the oppositely charged surfaces is especially pronounced at the distance between the charged surface being equal to the lengths of the dipoles, which is related to the bridging mechanism [44, 45].

In this paper, we considered the system of two oppositely charged planar surfaces in a solution composed of dipoles of arbitrary length and monovalent ions. The variational theory applied to the free energy of our system leads to the non-local integro-differential equation, which is also interesting from the mathematical point of view. In fact, the equation is a boundary value problem for an integro-differential equation, which has been considered for the first time and it cannot be fitted in known theories. The obtained numerical results help to understand the spatial and the orientational distributions of dipoles between two oppositely charged surfaces.

References

[1] Grosberg A Y, Nguyen T T and Shklovskii B I 2002 *Mod. Rev. Phys.* **74** 329
[2] Barlow D J and Thornton J M 1986 *Biopolymers* **25** 1717
[3] Cevc G 1990 *Biochim. Biophys. Acta* **1031** 311
[4] McLaughlin S 1989 *Annu. Rev. Biophys. Biophys. Chem.* **18** 113
[5] Lau A W C and Pincus P 1999 *Eur. Phys. J.* B **10** 175
[6] Parsegian V A and Gingell D 1972 *Biophys. J.* **12** 1192
[7] Alberts B, Johnson A, Lewis J, Raff M, Roberts K and Walter P 2002 *Molecular Biology of the Cell* (New York: Garland Science)
[8] Russ C, Heimburg T and von Grünberg H H 2003 *Biophys. J.* **84** 3730

[9] Crystal R G 1995 *Science* **270** 404
[10] Fleck C, Netz R R and von Grünberg H H 2002 *Biophys. J.* **82** 76
[11] Jackson J D 1999 *Classical Electrodynamics* (New York: Wiley)
[12] Cayre O, Paunov V N and Velev O D 2003 *J. Mater. Chem.* **13** 2445
[13] Snyder C E, Yake A M, Feick J D and Velegol D 2005 *Langmuir* **21** 4813
[14] Hol W G J, van Duijnen P T and Berendsen H J C 1978 *Nature* **273** 443
[15] Sheridan R P, Levy R M and Salemme F R 1982 *Proc. Natl Acad. Sci. USA* **79** 4545
[16] Rogers N K and Sternberg M J E 1984 *J. Mol. Biol.* **174** 527
[17] Verwey E J W and Overbeek J Th G 1948 *Theory of the Stability of Lyophobic Colloids* (New York: Elsevier)
[18] Evans D F and Wennerström H 1994 *The Colloidal Domain: Where Physics, Chemistry, Biology, and Technology Meet* (New York: VCH)
[19] Kjellander R and Marčelja S 1984 *Chem. Phys. Lett.* **112** 49
[20] Kjellander R and Marčelja S 1986 *J. Phys. Chem.* **90** 1230
[21] Attard P, Mitchell D J and Ninham B W 1988 *J. Chem. Phys.* **88** 4987
[22] Podgornik R 1990 *J. Phys. A: Math. Gen.* **23** 275
[23] Stevens M J and Robbins M O 1990 *Europhys. Lett.* **12** 81
[24] Kralj-Iglič V and Iglič A 1996 *J. Physique* **II 6** 477
[25] Borukhov I, Andelman D and Orland H 1997 *Phys. Rev. Lett.* **79** 435
[26] Bohinc K, Kralj-Iglič V and Iglič A 2001 *Electrochim. Acta* **46** 3033
[27] Bohinc K, Iglič A and May S 2004 *Europhys. Lett.* **68(4)** 494
[28] Guldbrand L, Jönsson B, Wennerström H and Linse P 1984 *J. Chem. Phys.* **80** 2221
[29] Moreira A G and Netz R R 2001 *Phys. Rev. Lett.* **87** 078301
[30] Bratko D and Vlachy V 1982 *Chem. Phys. Lett.* **90** 434
[31] Lamperski S and Outhwaite C W 1999 *J. Electroanal. Chem.* **460** 135
[32] Stillinger F H and Rahman A 1974 *J. Chem. Phys.* **60** 1545
[33] Lamperski S 1994 *J. Electroanal. Chem.* **373** 211
[34] Safran S A 2003 *Statistical Thermodynamics of Surfaces, Interfaces, and Membranes* (Colorado: Westview Press)
[35] Buijs J, White D D and Norde W 1997 *Colloids Surf.* B **8** 239
[36] Bergkvist M, Carlsson J and Oscarsson S 2001 *J. Phys. Chem. B* **105** 2062
[37] Porschke D 1985 *Biophys. Chem.* **22** 237
[38] Hiemstra T and van Riemsdijk W H 2006 *J. Colloid Interface Sci.* **301** 1
[39] Kirkwood J G and Shumaker J B 1952 *Proc. Natl Acad. Sci. USA* **38** 863
[40] Bratko D and Vlachy V 1985 *Colloid. Polym. Sci.* **263** 417
[41] Kallay N and Tomič M 1988 *Langmuir* **4** 559
[42] Huang H, Manciu M and Ruckenstein E 2003 *J. Colloid Int. Sci.* **263** 156
[43] Ninham B W and Parsegian V A 1971 *J. Theor. Biol.* **31** 405
[44] Podgornik R 2004 *J. Polym. Sci.* **42** 3539
[45] Meyer E E, Lin Q, Hassenkam T, Oroudjev E and Israelachvili J N 2005 *Proc. Natl Acad. Sci. USA* **102** 6839